Pattern Recognition 42 (2009) 2787 – 2796

Contents lists available at ScienceDirect

Pattern Recognition

journal homepage: www.elsevier.com/locate/pr

Use of random time-intervals (RTIs) generation for biometric verification

Nikolaos A. Laskaris*, Stefanos P. Zafeiriou, Lambrini Garefa

Artificial Intelligence & Information Analysis Laboratory, Department of Informatics, Aristotle University, GR-54124 Thessaloniki, Greece

ARTICLE INFO

Article history:
Received 11 September 2008
Received in revised form 11 December 2008
Accepted 23 December 2008

Keywords:
Authentication
Cognitive biometrics
Multivariate Wald-Wolfowitz test
Reconstructed dynamics

ABSTRACT

We explore the possibility of using human-generated time-series as biometric signature. Adopting a simple psychometric procedure, in which a button is pressed in entirely random manner, successive elapsed times are registered and gathered in a signal reflecting user's internal cognitive processes. By reconstructing and comparing the dynamics across repetitions from the same subject a noticeable consistency was observed. Moreover, the dynamics showed a prominent idiosyncratic character when realizations from different subjects were contrasted. We established an appropriate similarity measure to systematize such comparisons and experimentally verified that it is feasible to restore someone's identity from RTI (random time-interval) signals. By incorporating it in an SVM-based verification system, which was trained and tested using a medium sized dataset (from 40 persons), a considerably low *equal error rate* (EER) of ~5% was achieved. RTI signals can be collected effortlessly and this makes our approach appealing, especially in transactions mediated by standard pc terminal keyboards or even telephone keypads.

1. Introduction

The new era of Biometrics includes automated methods of recognizing a person based on a physiological or behavioral characteristic, like face, fingerprints, hand geometry, handwriting, iris, vein topography, and voice [1]. As the level of security breaches and transaction fraud increases, the need for highly secure identification and personal verification technologies is becoming apparent. Biometric-based solutions are able to provide for confidential financial transactions and personal data privacy. Utilizing biometrics for personal authentication is becoming convenient and considerably more accurate than current methods (such as the utilization of passwords or PINs). This is because biometrics links the event to a particular individual (a password or token may be used by someone other than the authorized user), is convenient (nothing to carry or remember), accurate (it provides for positive authentication), can provide an audit trail and is becoming socially acceptable and cost effective.

After the first wave of biometrics, which included static and naturally distinctive characteristics like the face and signature, researchers started to experiment with more dynamic characteristics like the voice or handwriting style (online/dynamic signature verification) which are more difficult to be imitated (e.g. [2]). Keystroke dynamics [3] also known as typing recognition, is a typical biometric approach of this kind. It analyses the way a person types. Users enroll by typing the same word or phrase a number of times [4]. Verification is based on the concept that the rhythm with which a person types is distinctive. It is an appealing approach since no extra hardware is required and typing is the most natural way for a user/client to interact with the system/server in most applications, particularly over the world-wide web. However, the passage to be typed might need to be fixed and this means a memory load, analogous to remembering an extra password. Moreover, there is a potential change due to continuous practice of the same typing patterns.

In the present paper we propose an alternative biometric in which the simplicity of interface is kept, while the restriction of typing specific patterns is alleviated. The present work was motivated by recent, independent studies in cognitive neuroscience and psychiatry reporting that the generation of random rhythms or numbers is a demanding cognitive task and carries enough information to discriminate between different clinical populations. When someone is asked to generate (verbally of via keyboard) random numbers, there is a cognitive load implied, since there is a close interaction between short-term memory and internalized decision making mechanisms [5–8]. A closely related task is the generation of random tapping rhythms [9,10]. Finger tapping, in particular, requires sensorimotor interaction and specific cortical networks responsible for this have been identified and modeled by Kelso [11,12]. Interestingly, it has been demonstrated that everyone has his own eigen-rhythms regulating spontaneous finger tapping [13].

Following a standard psychometric procedure [14–16], we gathered multiple RTI (random time-interval)-signals from a random

* Corresponding author. Tel.: +30 2310 998706; fax: +30 2310 998453.
E-mail address: laskaris@aiia.csd.auth.gr (N.A. Laskaris).

0031-3203/$ - see front matter © 2009 Elsevier Ltd. All rights reserved.
doi:10.1016/j.patcog.2008.12.028

group of subjects and systematize the inter-subject comparisons with respect to the dynamics governed the generation of the registered random-rhythms. Due to the non-stationary (and rather 'chaotic') character of the signals, neither standard spectral analysis nor traditional morphological analysis could provide us with useful discriminating characteristics. Nonlinear-dynamics, instead, enabled us to compare the underlying generation mechanisms directly based on the time-series (TS). Dynamic trajectories, when suitably reconstructed, were proved sufficient for building reliable biometric-tests.

The contribution of our paper is twofold. At an experimental level, it is the first time that human-generated TS of random latencies are tested as biometric. Moreover, at a more theoretical level, TS related to brain-event dynamics are compared in a novel way, namely by means of a non-parametric statistical test. The results from the extensive experimentation with a particular authentication-system (encompassing the introduced ideas) are highly encouraging, since the measured performance approximates the current standards in the field, without resorting to highly sophisticated registration procedures (like 3D scanners).

The paper is organized as follows. Section 2, describes the procedure for recording RTI-signals. Section 3 is devoted to the novel pairwise comparison of such signals. Section 4 describes a possible way to transform these pairwise comparisons to discriminant-functions. Section 5 outlines a specific verification system, while Section 6 includes a detailed evaluation. The final section includes a short discussion and some comments on a more beneficial implementation of our suggested-methodology.

2. The random rhythm generation test

The procedure for generating the RTI signals is very simple [14–16]. The subject is asked to press the space key of the computer with the index finger of his/her dominant hand as irregularly as possible, until the screen shows the end of the exercise. The first time the subject encounters this task, he/she is provided beforehand with an example consisting of a square 4×4 cm, which appears and disappears in the screen at random rhythm and is synchronized with a sequence of beeps. The particular example is indicative of the sort of TS he has to create and—as it is explicitly stated—its exact reproduction is not the objective of the task. If $x(t)$ denotes the T-length sequence of exact time-latencies of subject's blows $\chi[n]=[t_1,t_2,\ldots,t_T]$, the corresponding RTI signal takes the form $x[n]=[t_2-t_1,t_3-t_2,\ldots,t_T-t_{T-1}]$. During the enrolment-stage, such a $\chi[n]$ sequence is provided by the user and the RTI signal (i.e. the sequence of latency-differences) is automatically created and compared with analogous ones previously stored in the database of the system. This comparison should reflect as much as possible the inter-user differences regarding the internalized process of generating random rhythms. On the other hand, someone's mechanism was expected to remain the same and this constancy should be apparent, as well, in the temporal characteristics of his RTI-signals measured repeatedly. Fig. 1a, includes a few examples of RTI-signals recorded from three different subjects.

3. Comparing the reconstructed dynamics

Since, the ultimate goal was to contrast the underling dynamics by means of comparing the corresponding TS, we resorted to techniques from nonlinear dynamics field [17]. In our approach we, first, reconstruct the dynamics from each TS as a trajectory in a suitable chosen state-space of high dimensions and then compare these trajectories—in pairs—via a powerful non-parametric multivariate-statistical test [18,19].

Using Taken's *time-delay embedding* procedure [20], a succession of delay-vectors $\mathbf{x_i}(n)=(x[n-(p-1)\times\tau],\ldots,x[n-\tau],x[n])$ is first formed from each RTI-signal $x_i[n]$ and them listed in a matrix $\mathbf{X}=[\ldots\mathbf{x_i}(n-1)|\mathbf{x_i}(n)|\mathbf{x_i}(n+1),\ldots]$. In this formulation the parameter p is the *embedding dimension*, i.e. the dimensionality of reconstructed state-space and τ is the so-called *time-lag* parameter [17]. The former is usually selected high enough so that the degrees of freedom of the dynamical system are preserved. The latter is usually defined so as to decorrelate the successive components of the formed vectors. The matrix $\mathbf{X}$ tabulates the dynamical orbit related with the generation mechanism of the RTI-signal. Fig. 1b, demonstrates two such trajectories reconstructed (with $\tau=5$ and $p=2$) from RTI-signals of Fig. 1a. The systematic comparison between any two such trajectories $\mathbf{X}$ and $\mathbf{Y}$ resulting from time-delay embedding is a relative unexplored task and only recently a few methodologies have been introduced [21–24]. Motivated by our own previous work, where we had compared trajectories related to brain-response dynamics [25,26], we adopted the statistical procedure of multivariate Wald-Wolfowitz (WW-test) which is described in some detail in Appendix B. In short, using two sets of delay-vectors $\{\mathbf{x_i}\}$ and $\{\mathbf{y_i}\}$ (tabulated correspondingly in matrices $\mathbf{X}$ and $\mathbf{Y}$) the overall *minimal spanning tree* (MST) graph is constructed (see Appendix A) and the W statistic quantifies if the different branches of MST are populated equally by the two sets of vectors. W is computed based on the encountered combinatorics and used as a measure expressing the similarity between the dynamics of RTI-signals $x[n]$ and $y[n]$. The more positive the value $W(x[n],y[n],\tau,p)=W(\{\mathbf{x_i}\},\{\mathbf{y_i}\})$, the more similar the two trajectories are. The function of WW-test is demonstrated in details via Fig. 1c, where RTI-signals from two different subjects are contrasted. It is clear that WW-test practically takes into account the relative overlap of the corresponding trajectories. Hence the W-index is a symmetric measure, i.e. $W(x[n],y[n],\tau,p)=W(y[n],x[n],\tau,p)$. Due to the non-parametric character of the employed test, this index has a generic character when used as a similarity measure for comparing the dynamics from two different TSs. The only restriction is that the embedding parameters p and τ should be the same for the two signals. It can easily be understood that WW-test can compare signals of different length and simultaneously ignore differences due to relative latency jitter (i.e. it is translation invariant). Moreover, since the W-index springs from an appropriate standardization (see Eq. (B.3)), it carries an absolute meaning and, hence, can be compared across different embeddings of the same RTI-signals. This particular option can be utilized, as it described below, to optimize the selection of the two involved parameters (τ, p).

4. Classifying the reconstructed dynamics and optimizing the embedding

Having introduced the similarity measure $W(x[n],y[n],\tau,p)$ between any two RTI-signals $x[n]$ and $y[n]$, we proceed by describing the way the adopted similarity measure can be utilized in establishing classifiers, the core-machinery in any biometric-system. For a given set of available RTI-signals $x_i[n]$, $i=1,\ldots,N$ with known identity, we compute all pairwise similarities and tabulate them, after a simple transformation, in an $[N\times N]$ distance-matrix $\mathbf{D}$ with elements

$$[D]_{i,j}=D(i,j)=\begin{cases}0 & W(x_i[n],x_j[n],\tau,p)>0\\ \mathrm{abs}(W(x_i[n],x_j[n],\tau,p)), & \text{otherwise}\end{cases} \quad (1)$$

Since the majority of classifiers operate on vectorial data, the above relational data are transformed to coordinate vectors via multidimensional scaling (MDS), a spectral technique that results to N vectors $g_i\in R^l$ such that the interpoint Euclidean distances $\|g_i-g_j\|$ approximates as much as possible the tabulated ones $[D]_{i,j}$. The MDS operation is signified as $\mathbf{G}=\mathrm{MDS}(\mathbf{D},l)$, with l denoting the output

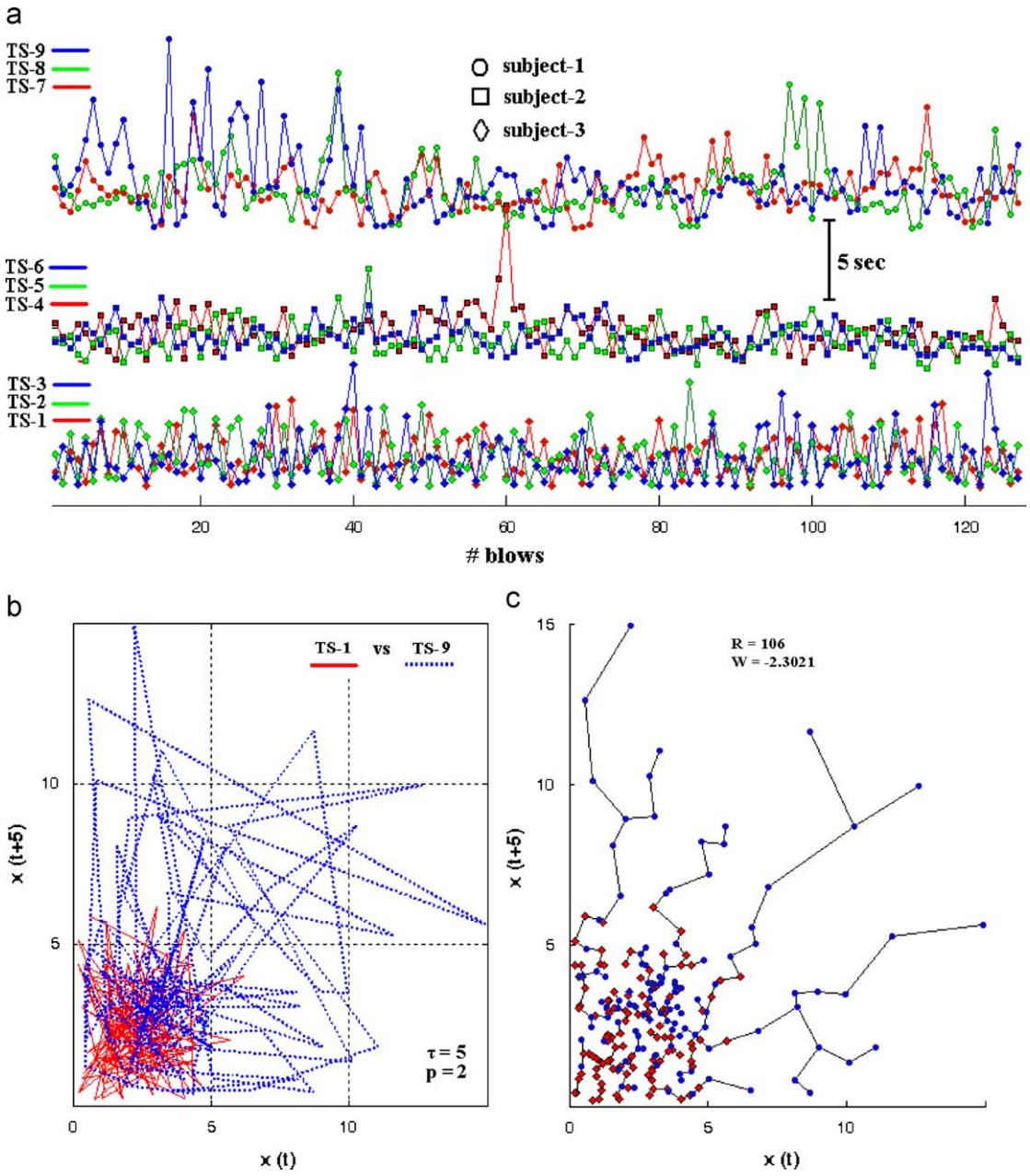

Fig. 1. From RTI-signals to similarity-relations: (a) multiple RTI-signals from three different subjects; (b) superposition of two reconstructed ($\tau = 5$, $p = 2$) trajectories; and (c) using the WW-test for measuring the similarity between the two given trajectories.

dimensionality [26]. The quality of this approximation is measured via the discrepancy

$$Stress = \frac{\sum_{i<j}^{N} |D(i,j) - \|g_i - g_j\||}{\sum_{i<j}^{N} D(i,j)} \tag{2}$$

A stress value lower than 0.15 denotes a configuration, which can be considered a faithful representation of the provided dissimilarities. As l increases, the stress decreases and this succession can be used to select the optimal representation-dimension. Fig. 2, exemplifies the above described procedures using the RTI-signals from Fig. 1a. The left-panel provides a visualization of the Distance-matrix corresponding to WW-test applied with $p = 2$ and $\tau = 5$. The successive value of stress, shown in the middle-panel, indicate (according to the 'elbow-rule') that $l = l_o = 2$ is sufficient. The right panel provides the MDS-based 2D coordinate representation of the Distance-matrix. In this plot, the RTI-signals appear as distinct points with labels [1–9] and colors in full accordance with the ones used in Fig. 1a. From the stress-index value is evident that this point-sample provides a reliable representation regarding the dynamics of the RTI-generation mechanism. Taking into consideration the given classification (i.e. the labels denoting the subjects' id), it is apparent that RTI-signals treated with our approach reflect enough information to discriminate the involved subjects and therefore a classifier could be easily built in the MDS-based representation-space. To quantify more precisely this apparent inter-subject differentiation, we employed a functional **J** that expresses the ratio between the *between-group scatter* (an aggregate measure of differences between TSs from different subjects) and the *within-group scatter* (the aggregate difference between TSs from the same subject). The form of this

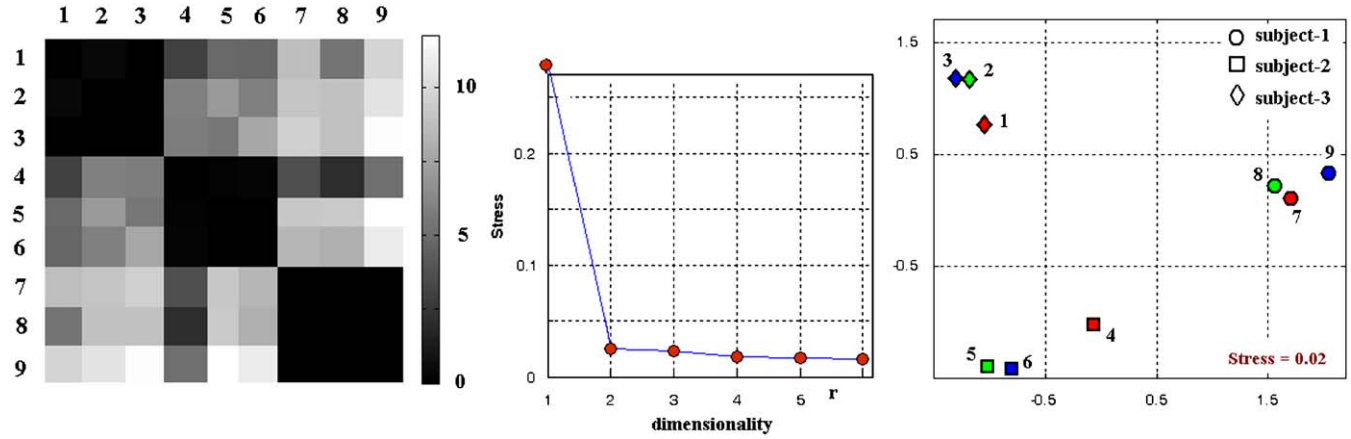

Fig. 2. From the original relational data (corresponding to all the WW-related pairwise comparisons among the RTI-signals of Fig. 1a) to their 2-D representation using MDS. Similar signals are mapped to nearby points.

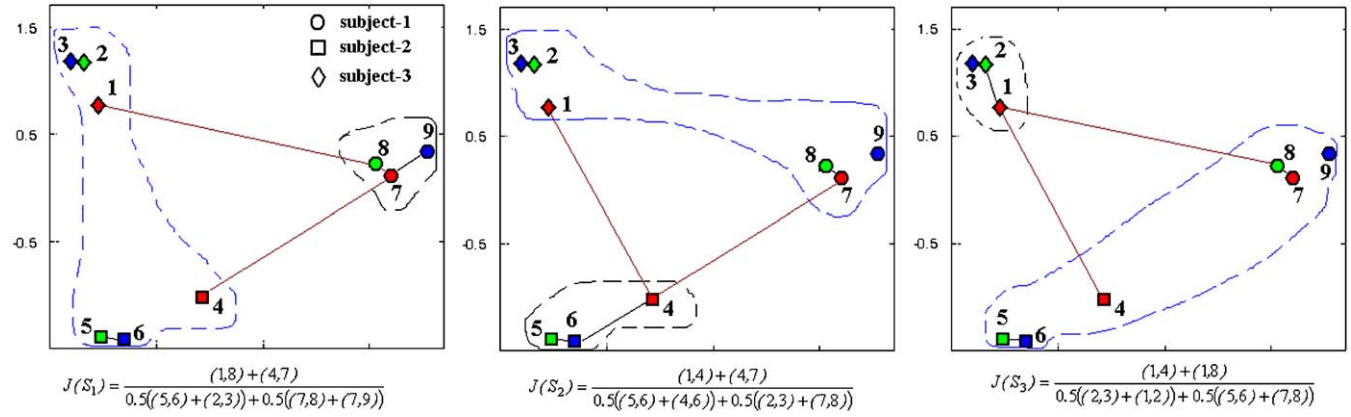

Fig. 3. Quantifying the separability among three different subjects based on the WW-related comparisons between their RTI-signals (originally shown in Fig. 1a).

functional was borrowed from the *Fisher-analysis* literature and properly translated for the particular scenario in which only dissimilarities $D(x_i[n],x_j[n])$ are available between the RTI-signals. We introduce the functional **J** using Fig. 3 to conceptualize the employed measures, but it can straightforward be generalized for arbitrary number of subjects and RTI-signals per subject (a similar formulation has been provided recently in [27]). Put it in words, for each subject in turn its own TSs are considered as forming one group and all the rest TSs as forming a single, complementary group. For both groups the k nearest neighbors among the members of the same group are identified and the corresponding distances are summed to express the *within-scatter* (*WS*). In the same way, the k-nearest neighbors belonging to opposite groups are recognized and the corresponding distances are summed to provide *inter-scatter* (*IS*). By averaging the ratios IS/WS estimated for all subjects, we provide the net class-separability $\mathbf{J}=\mathbf{J}(\mathbf{D},\mathbf{k})$

$$\mathbf{J}=\mathbf{J}(\mathbf{D},\mathbf{k})=\frac{1}{3}\sum_{i=1}^{3}J(S_i,k)=\frac{1}{3}\sum_{i=1}^{3}\left(\frac{IS}{WS}\right)_i \tag{3}$$

For the particular instantiation of Fig. 3, the number of neighbors was set to $k=2$ and J was found $\mathbf{J}(\mathbf{D},\mathbf{k}=\mathbf{2})=7.1$. In general, values significantly higher than 1 denote sufficient inter-subject discrimination. In this work we utilized the J functional as a gauge to guide the selection of the two embedding parameters τ and p. During the preliminary stage of the authentication-system development, we experimented with different values for the two parameters and formed

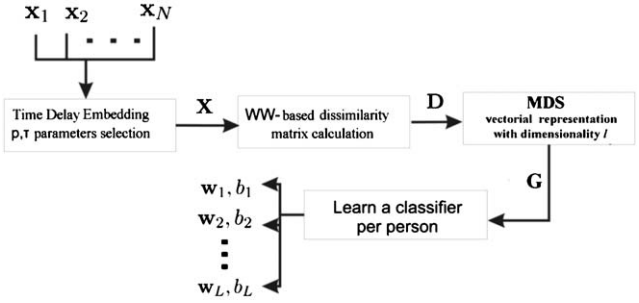

Fig. 4. Schematic diagram of the training procedure for the SVM-based verification system.

the corresponding distance-matrices $D_{\tau,p}$. By identifying the maximum of $J(D_{\tau,p},k)$ over the range of tested parameters, we decided for the optimal embedding that could facilitate the best performance in the subsequent training of the classifier (see Fig. 4). In other words, our approach is reminiscent of the *filter*-procedure (rather than the *wrapper*-approach) used for feature selection in classifiers design.

5. The SVM-based verification system

We provide here an outline of the employed verification system. It builds over the *minimum class variance support vector machine*

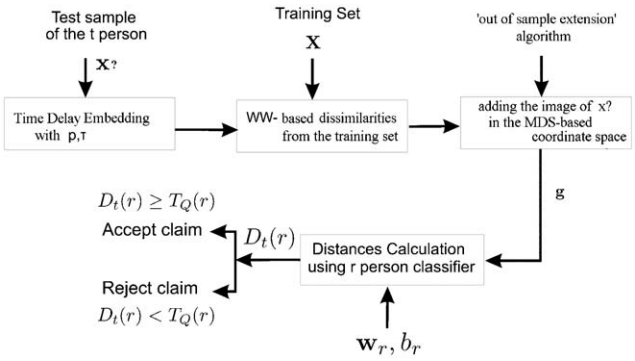

Fig. 5. Schematic diagram of the testing procedure for the SVM-based verification system.

(MCVSVM). Details for the classifier and its training can be found in [28]. A short description can be found in Appendix C. Following the standard distinction between the training and the test/claim stage, we list below the corresponding algorithmic steps (and schematically present them in Figs. 4 and 5).

Training stage:

(i) Build the database with N RTI-signals from the L users $x_i[n]$ (each user should provide multiple signals).
(ii) Select the embedding parameters p,τ (preliminary stage), apply WW-test and derive $D_{p,\tau}$ using Eq. (1).
(iii) Via spectral analysis, derive a vectorial representation $\mathbf{G} = \mathrm{MDS}(\mathbf{D},l)$ for the set of N signals using variable dimensionality l and select the optimal l_o based on the stress-value. In our particular implementation, this representation goes beyond classical MDS [31], as it is discussed in the Supplementary material.
(iv) Using this optimized vectorial representation (i.e. the g_i vectors, $g_i \in R^{l_o}$), train the SVM-system. For each user, a decision function in computed (see Eq. (C.5) in Appendix C).

Test/claim stage:

(i) For an unknown person that claims to be one of the L users, in particular the r-th client, collect T successive latencies and construct a single RTI-signal $z[t]$.
(ii) Apply WW-test between the new RTI-signal and those in the database, i.e. compute $\mathrm{WW}(z[n],x_i[n])$, $i = 1,\ldots,L$ and transform these to dissimilarities using Eq. (1).
(iii) Use the 'out of sample Extensions' (see [29,30] and the supplementary material), to 'project' the new RTI-signal $z[n]$ in the MDS-based coordinate space.
(iv) Apply the decision-function corresponding to the r-th user on the appended image of $z[n]$.

6. Experimental procedure—evaluation of the verification system

6.1. The data

Forty (18/22 males/females) age-matched subjects (age: 23 ± 3 yrs) participated in this initial study. Each participant was employed in the generation of 10 RTI-signals in five different recording days. A couple of random-latency signals, consisting of $T = 128$ blows each, were recorded every time. Between the two TS recorded within the same appointment, a different task was offered to the participant (either a constant-time interval generation task, or a short session of a computer game). All the measurements were carried with the same software developed for Matlab-platfom, but using five different computers (with similar settings for the keyboards connected to PS/2 port) placed in two different laboratories. Subjects were assigned randomly to laboratories and computers and in way that a particular subject never used the same computer for two consecutive recording appointments. The recording time of a single TS, on average, lasted 175 ± 35 s.

6.2. The optimal embedding

Using all the RTI-signals we first searched for the optimal embedding parameters. Following the procedure described in Section 4, we varied p and τ giving rise to a graph (not shown here) in the form shown in Fig. 6. In the particular graph of Fig. 6, the original values of **J** functional have been transformed to *z-scores* based on a randomization test [32] (which included 1000 random permutations of the tabulated RTI-signals, the corresponding derivations of J-value, and the final computation of mean and standard deviation of all these intermediate J-values). It is easy to notice that for the wide range of embedding parameters, person-recognition/identification based on RTI-signals appears a feasible task. Moreover, the shown curve was suggestive of using two different pairs for the embedding parameters: ($\tau = 1$, $p = 7$) and ($\tau = 3$, $p = 4$). For both cases the 'elbow rule' provided that a vectorial representation in a coordinate space of $l_o = 10$ dimensions was sufficient for encompassing the comparisons between all the RTI-signals and building the SVM-verification system within.

6.3. The parameter tuning of the verification system(s)

To fully validate our suggestion, we adopted a standard experimental protocol and use it to validate the function of MCVSVM-system presented in Section 5. To further demonstrate that the RTI-signals convey discriminative information that can be captured by simpler verification systems as well, we measured the performance of alternative verification systems as well (including a simple thresholding scheme and a standard SVM algorithm [33,34]). In the followings, we refer to the employment of all these alternatives as different verification scenarios. The common protocol used for every verification scenario was the following. Five experimental sessions were implemented by employing the leave-one-out (jackknife) and rotation estimates. In each session, two samples were left out to be used as a test set. To implement test impostor claims, we rotated over the 40 person identities by considering the samples of each person in the test set as an impostor. By excluding any sample of the test impostor from the remaining four sessions, a training set consisted of 39 clients was built. The test impostor pretended to be one of the 39 clients and this attempt was repeated for all client identities. As a result, 39×2 impostor claims were produced. In a similar manner, 39×2 test client claims were tested by employing the clients' samples from the session that was left out and those of the training set. Let $A1,A2,A3,\ldots,A40$ be the identity codes of the persons included in the database. Fig. 7 depicts the experimental protocol when person $A1$ is considered to be an impostor and the samples of Session 5 is employed as test set. It can be seen that the training set is built of four out of the five available sessions each one consisted of 39 out of the 40 available persons. The comparisons shown for person $A1$ are repeated for all other persons in the database. Obviously, similar comparisons are made by rotating among the available sessions.

Next, we describe the training procedure. It is applied to the training set of the 39 clients. For each client, we had 8 samples at our disposal. Let us assume that person $A1$ using one of his two samples from Session 5 pretends to be person $A2$ during the test procedure. To test such a claim, we first implement the training stage, which—depending on the verification scenario—includes: (i) the

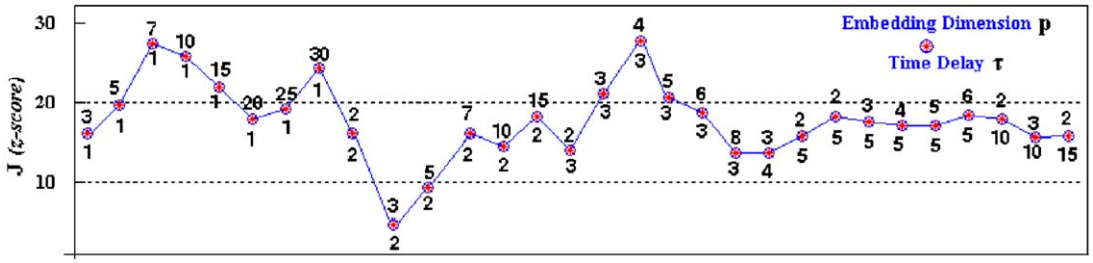

Fig. 6. Class-separability **J** as a function of the two embedding parameters.

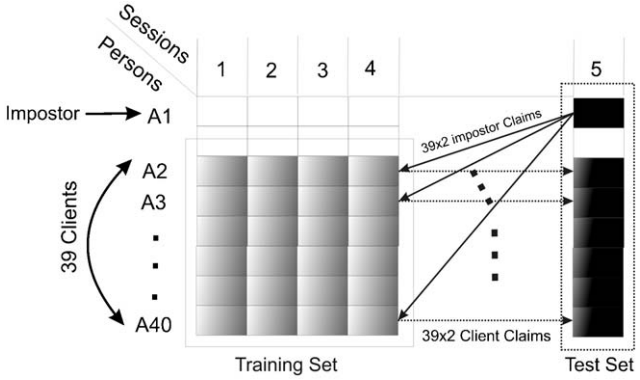

Fig. 7. The experimental protocol.

computation of WW-test scores and their transformation to dissimilarities; (ii) the vectorial representation of all the pairwise comparisons among RTI-signals and the subsequent computation of L2-norm distances (here MDS acts as a 'denoising' step); (iii) the derivation of optimal separating hyperplane for every person so that the margin is maximized (i.e. SVMs [33,34]) and the construction of a decision functions; and (iv) the derivation of optimal separating hyperplane for every person so that the within-class variance is minimized (i.e., MCVSVMs [28]), and the construction of a decision functions.

In all the previous scenarios, the derivation of a decision-threshold is included as a common training step.

For the last two cases the distance to the optimal separating hyperplane is used as the measure to be compared against the optimized threshold. On the contrary, in the former two cases the WW-related scores are submitted to thresholding. In all cases the defined thresholds should ideally enable the distinction between the distance measures that correspond to client claims within the trained class under study and the distance measures that correspond to impostor claims for impostors that belong to any other class. In the instantiation of Fig. 7, the training procedure determines and 39 thresholds T_{Ai} (and 39 pairs of separating hyperplanes $(w_{Ai};b_i)$ in the case of the last two verification-scenarios). Let us now explain how these thresholds are defined and incorporated in the final decision. For clarity purpose, we consider the case of person $A1$ being an impostor and persons $A2,\ldots,A40$ being clients. We assume that person $A1$ uses one of his samples to pretend to be person Ar. When using only the WW-test related dissimilarity measure (i.e. the first verification scenario) between the samples, we employ the method proposed in [35] for threshold calculation. According to this, the dissimilarity measures for every person calculated in the training set are used to form the distance vector $\mathbf{o}(\boldsymbol{r})$. The elements of the vector $\mathbf{o}(\boldsymbol{r})$ are sorted in ascending order and are used for the *person specific thresholds* on the distance measure. Let $TQ(r)$ denoting the Q-th order statistic of the vector of distances, $\mathbf{o}(\boldsymbol{r})$. The threshold of the person r is chosen to be equal to $T_Q(r)$. Let $r1,r2,\ldots,r8$ be the 8 instances of the person r in the training set. A claim of a person t is considered valid if $\min_j\{D_t(r_j)\} < T_Q(r)$ where $D_t(r_j)$ is the distance between the sample of test person t and the reference sample r_j. In the rest three verification scenarios, we proceed in a similar way for the threshold calculation.

6.4. Performance evaluation

The performance of verification systems is measured in terms of the *false rejection rate* (FRR) achieved at a fixed *false acceptance rate* (FAR). There is a trade-off between FAR and FRR. That is, it is possible to reduce either of them with the risk of increasing the other one. This trade-off between the FAR and FRR can create a curve where FRR is plotted as a function of FAR (while altering the threshold value). This curve is called *receiver operating characteristic* (ROC) curve [36,37]. The performance of a verification system is often quoted by a particular operating point of the ROC curve where FAR = FRR. This operating point is called *equal error rate* (EER).

In the first scenario we have used only the WW-test scores for verification and adopted two different threshold politics. In the first one we have used *global thresholds* (GT) (i.e. common) for all the clients. In this case, since the WW-related scores range between 0 and 20 we have created 1000 successive thresholds between these values. In the second one we have used a threshold politic as described above (Section 6.3) and in [38]. The obtained ROC curves for the two different embeddings can be found in Fig. 8. As can be seen the *person-specific threshold* (PST) strategy gave the better results (i.e. lower EER). This was a common trend in all the verification scenarios, and for this reason in the performance measures reported hereafter, person-specific thresholds are everywhere implied.

Next we measured the verification performance corresponding to the previous verification scenario as a function of the total number of blows T. As can be seen in Fig. 9, the EER almost monotonically decreases with the number of RTI encountered.

Fig. 10 includes the performance measures for the 3rd and 4th verification scenarios as a function of the degree of polynomial kernel (Eq. (C.4)). A verification system based on a standard SVM algorithm [33,34] is compared with the MCVSVM system described in Section 5. The EER versus the degree of the polynomial kernel used is plotted for both SVMs and MCVSVMs in Fig. 10. As can be seen the employment of SVMs greatly enhances the verification performance. Both systems achieved their highest performance with the degree $d = 3$. MCVSVMs achieved the best EER that is 5.4%.

Fig. 11 includes the ROC curves from all verification scenarios overlaid, while Table 1 lists the corresponding EER. The performance of MCVSVM-based system is very satisfactory. We can easily prove that our test set is capable for providing such a measurement in statistical significant manner, by using a similar analysis with the one presented in [35]. That is, since a similar circular protocol has been used in [35] with 37 clients and 1 sample per session (we have more clients and two samples per session) we may accept, with safety, an *EER* 5%.

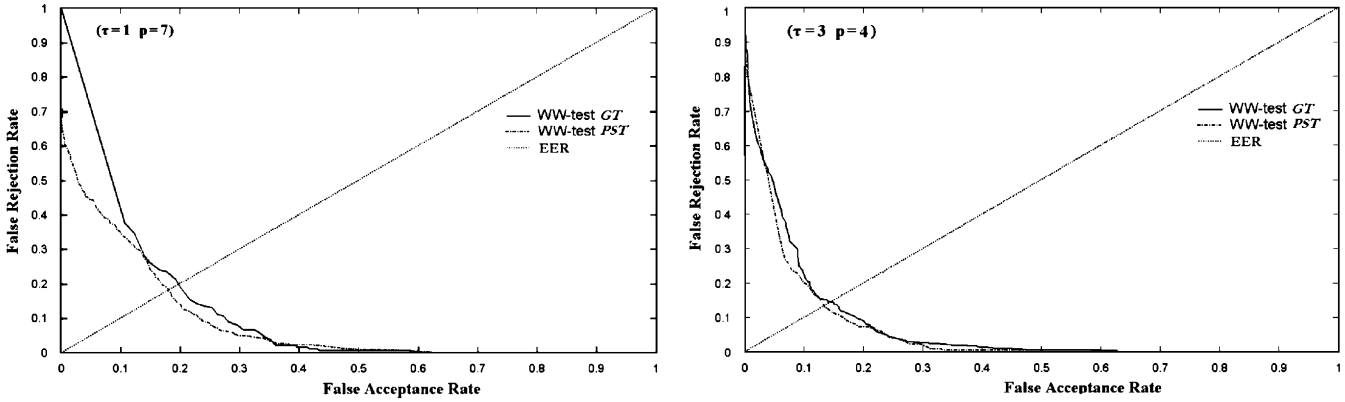

Fig. 8. ROC curves for Global and Person Specific Thresholds using simply the WW-based dissimilarity as the distance measure. Left/Right panel corresponds to the particular selected pair, shown in the left top corner, of embedding parameters (τ, p).

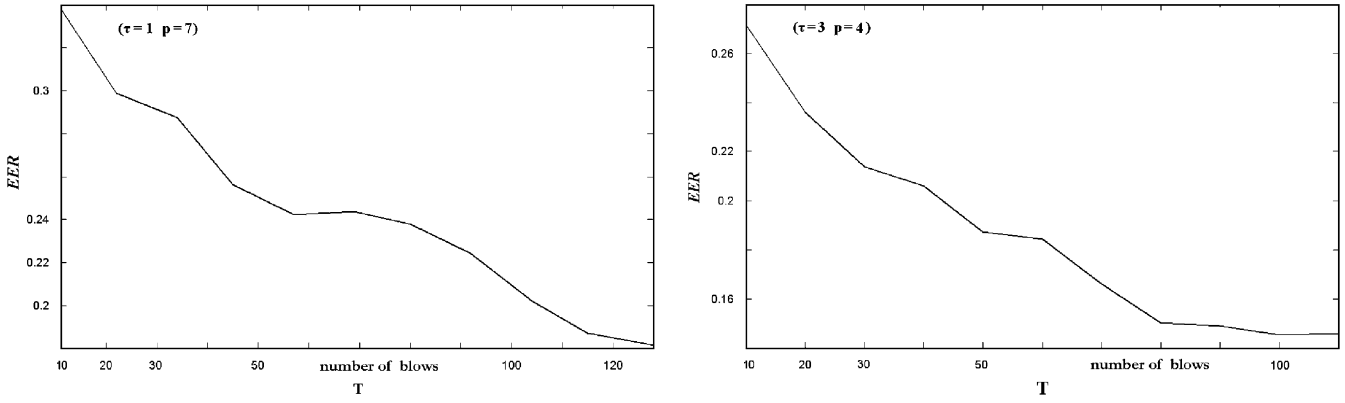

Fig. 9. EER for the PST-scheme as a function of the total number of recorded latencies. Left/Right panel corresponds to the particular selected pair, shown in the left top corner, of embedding parameters (τ, p).

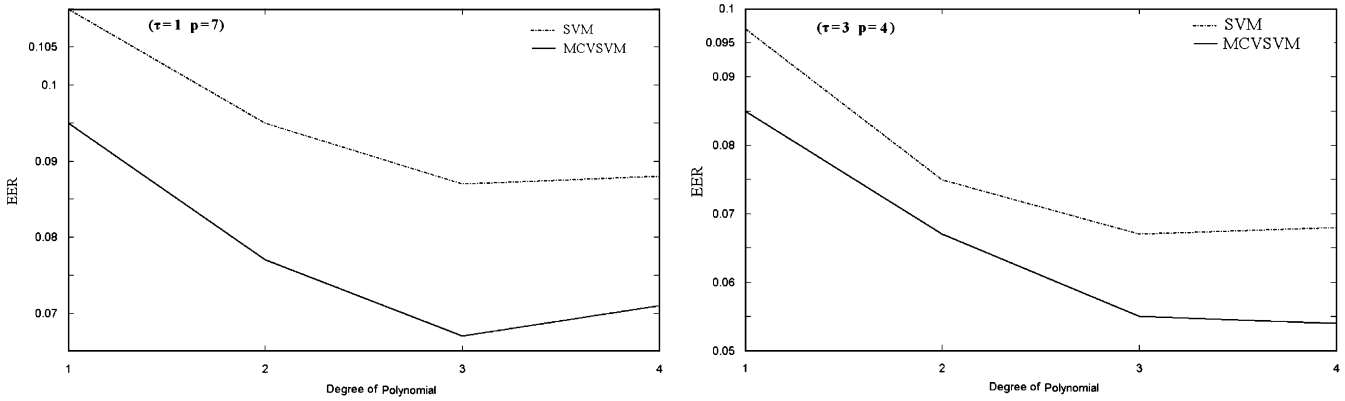

Fig. 10. The EER as a function of the degree of the polynomial kernels for the two SVM-related verification scenarios.

7. Discussion

A novel biometric was introduced that could be best described as cognitive, since it depends on higher brain functions that can be indirectly measured in a surprisingly simple way, Viz. the repetitive pressing of a button in a random manner. The signal of the registered time intervals was found to encode the person's identity and, therefore, could be used as a dynamic signature impossible to be imitated.

These ideas were tested on a medium sized database (10 signals from each of 40 persons). In a preliminary stage of the analysis (not included here), we experimented with various signal characteristics (i.e. features), like spectral descriptors and statistical moments. However, the inter-person separation was not sufficiently high. To overcome this shortcoming—and considering the 'chaotic nature' of the recorded signals—we borrowed form the field of nonlinear dynamics the idea to contrast the underlying mechanisms generating

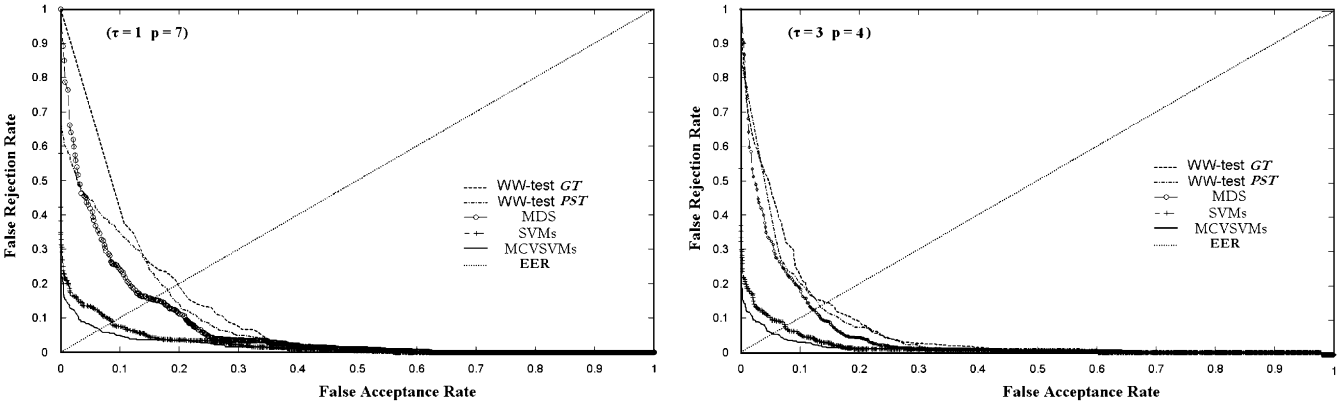

Fig. 11. A comparison of the ROCs for all the verification-scenarios. Left/Right panel corresponds to the particular selected pair, shown in the left top corner, of embedding parameters (τ, p).

Table 1
EER(%) for all verification scenarios.

EER (%)	1st Embedding $\tau = 1$, $p = 7$	2nd Embedding $\tau = 3$, $p = 4$
WW-test GT	19.80	14.51
WW-test PST	18.05	13.35
MDS ($l_o = 10$)	15.42	12.35
SVMs	8.80	7.55
MCVSVMs	6.51	5.40

these TS. These mechanisms were anticipated to be idiosyncratic and, consequently, distinguishable based on the associated reconstructed trajectories. The between-trajectories similarity was estimated by means of a flexible statistical test and the estimates were fed in different verification-systems, of varying complexity. The measured performance reached the EER-lever of 5%, which is very encouraging considering the convenience in taking such measurements and the apparent advantages of dealing with 1D signals. Even the simplest of the tested verification systems (i.e. a naive thresholding scheme, see Fig. 11), achieved a reasonable performance indicating that there is inherent, potentially useful information in this kind of signals when casted in the form of reconstructed dynamics. Spectral analysis (eigen-analysis) can help in revealing this information (see Fig. 11, MDS-curve), while sophisticated classifiers (see Fig. 11, SVM and MCVSVM curves) can fully exploit it. Therefore, our suggested biometric can be added to the battery of known dynamic signatures inspired by human physiological functions [39–46].

A noteworthy practical issue is the sufficient number of blows to be registered. It would be convenient if the highest performance could be achieved with the least possible engagement of the user (i.e. during verification, the user should accomplish the psychometric task in a very short time period). This issue has been addressed via Fig. 9. It can be seen that performance is kept increasing with the number of blows T. However, the right panel indicates that with $T = 80$ the maximum performance has, almost, been reached already. Considering that $T = 120$ corresponds to an average duration of 175 s, it is easily deduced that the random-interval generation task is time consuming. The most straightforward way to alleviate this is to keep the number of blows high when the person enrolls for the first time in the system (i.e. when he provides signals for building the training-test) and to reduce this number during the testing stage. Fortunately, our verification-system(s) inherits from the WW-test the necessary flexibility (since WW-test can readily compare TS of different length). Under this perspective, an alternative appealing research direction is the incorporation of recently introduced tactics from 'anytime-algorithms' theory [47,48], with the aim to avoid collecting random-intervals beyond the number necessary for the system to reach a secure decision.

The introduced method should be further justified based on a larger dataset. The nature of the new biometric signature (that enables registration remotely) can be fully exploited with the set up of a server that centralises the collection of RTI-signals via WWW. Moreover, a valuable methodological advancement is the incorporation of a test that will indicate the appropriate execution of the task and prompt its repetition whenever RTI-generation degenerates into isochronous tapping.

Appendix A. An introduction to MST graph

Graph theory sketches the MST structure with the following definitions. A *graph* is a structure for representing pairwise relationships among data. It consists of a set of *nodes* $V = \{V_i\}_{i = 1:N}$ and a set of links $E = \{E_{ij}\}_{i \neq j}$ between nodes called *edges*. The *degree* d_i of a node is the number of edges incident to it. When a weight e_{ij} is assigned to each link, a weighted-graph is formed and in the particular case that $e_{ij} = e_{ji}$ this graph is called *undirected weighted graph*. A *tree* is a connected graph with no cycles. A *spanning tree* T of a (connected) weighted graph $G(V,E)$ is a connected subgraph of $G(V,E)$ such that: (i) it contains every node of $G(V,E)$ and (ii) it does not contain any cycle. The *MST* is a spanning tree containing exactly $(N-1)$ edges, for which the sum of edge weights is minimum.

Appendix B. The multivariate Wald-Wolfowitz test (WW-test)

Given two multidimensional point samples $\{\mathbf{x_i}\}_{i = 1:m}$ and $\{\mathbf{y_i}\}_{i = 1:n}$, the hypothesis H_o to be tested is whether they are coming from the same multivariate distribution. At first, the sample identity of each point is not encountered and the MST of the overall sample is constructed. Then, based on the sample identities of the points, a test statistic R is computed. R is the total number of *runs*, while a *run* is defined as a consecutive sequence of identical sample identities. Rejection of H_o is for small values of R. The null distribution of the test statistic has been derived, based on combinatorial analysis [19].

Consider samples of size m and n, respectively, from distributions F_x and F_y, both defined in $\mathbf{R^P}$. Let $N = m+n$, C be the number of edge pairs of MST sharing a common node and d_i be the degree of the ith node. Under H_o, the mean and variance of R can be calculated as follows:

$$E[R] = \frac{2mn}{N} + 1 \tag{B.1}$$

$$Var[R|C] = \frac{2mn}{N(N-1)}\left\{\frac{2mn-N}{N} + \frac{C-N+2}{(N-2)(N-3)}[N(N-1)-4mn+2]\right\} \quad \text{(B.2)}$$

It has been shown that the quantity:

$$W = \frac{R-E[R]}{\sqrt{Var[R]}} \quad \text{(B.3)}$$

approaches (asymptotically) the standard normal distribution while $E[R]$ and $Var[R]$ are given in closed form based on the size of the two samples [19]. This enables the computation of the significance level (and p-value) for the acceptance of the hypothesis H_0.

Appendix C. The classifier built over the spectral-analysis based representations

Let r be the reference person. The MCVSVM classifiers are defined in the space of vectors g_i as the one that optimizes the following:

$$\min_{w_r,b_r,\xi} \frac{1}{2}\mathbf{w_r}^{\mathrm{T}}\mathbf{S}_w^r\mathbf{w_r} + C\sum_{j=1}^{N}\xi_j \quad \text{(C.1)}$$

Subject to the constraints:

$$y_i(\mathbf{w}_r^{\mathrm{T}}\phi(\mathbf{g_i}) + b_r) \geqslant 1-\xi_i \quad \text{(C.2)}$$

The within-class scatter $\mathbf{S}_w^r$ for the vectors g_i is defined as

$$\mathbf{S}_w^r = \left(\sum_{\mathbf{g_i}\in U_r}(\mathbf{g_i}-\mathbf{m_{U_r}})(\mathbf{g_i}-\mathbf{m_{U_r}})^{\mathrm{T}} + \sum_{\mathbf{g_i}\in \overline{U}_r}(\mathbf{g_i}-\mathbf{m_{\overline{U}_r}})(\mathbf{g_i}-\mathbf{m_{\overline{U}_r}})^{\mathrm{T}}\right) \quad \text{(C.3)}$$

where U_r is the set of the client samples for the reference person r and $\overline{U}_r$ of the impostor samples, while $\mathbf{m}$ denotes the mean vector computed for the corresponding class. Moreover, in constraints (C.2) y_i is the label of vector $\mathbf{g_i}$ (i.e., $y_i=1$ if $\mathbf{g_i}\in U_r$ and $y_i=-1$ if $\mathbf{g_i}\in\overline{U}_r$), $\xi=[\xi_1,\xi_2,\ldots,\xi_N]$ is the vector of slack variables associated with the allowed error, C is a given constant that defines the cost of the errors after the classification and φ is a nonlinear mapping that allows the design of the nonlinear surfaces. In SVM theory it is not necessary to have the closed form of the mapping $\varphi:R^{\mathrm{I}}\rightarrow F$ and we only need the closed form for the dot product $k(\mathbf{x},\mathbf{y})=\varphi(g_i)^{\mathrm{T}}\varphi(\mathbf{g_j})$ also known as kernel. Specifically, we have used polynomial kernels:

$$k(\mathbf{x},\mathbf{y}) = \varphi(x)^{\mathrm{T}}\varphi(y)^{\mathrm{T}} = (\mathbf{x}^{\mathrm{T}}\mathbf{y}+1)^d \quad \text{(C.4)}$$

where d is the degree of the polynomial. The above constrained optimization problem using positive kernels is solved as described in [28,33,34] or using widely available optimization packages.

Let that a test sample (i.e. a RTI-signal not known during training) arrives for testing, then it is 'projected' in the representation space (using the dissimilarities with the users' RTI-signals) and represented via a new vector $\mathbf{g}$. To test whether or not $\mathbf{g}$ belongs to the r-th client class, the following function is employed:

$$f(\mathbf{g}) = \mathbf{w}_r^{\mathrm{T}}\phi(\mathbf{g}) + b_r \quad \text{(C.5)}$$

with $\mathbf{w_r}$ and b_r client specific parameters computed during the training. The calculation of term $\mathbf{w}_r^{\mathrm{T}}\phi(\mathbf{g})$ is performed using the kernel function (C.4). The value of $f(\mathbf{g})$ is used as a measure of similarity by the verification system. The more positive, the more probably that the test sample is from the r-client. This value will be compared against an optimized threshold for the final decision made by the verification system.

Appendix D. Supplementary material

Supplementary data associated with this article can be found in the online version at 10.1016/j.patcog.2008.12.028.

References

[1] A. Jain, A. Ross, S. Pankanti, Biometrics: a tool for information security, IEEE Transactions on Information Forensics and Security 1 (2) (2006) 125–143.
[2] A. Jain, F. Griess, S. Connell, On-line signature verification, Pattern Recognition 35 (12) (2002) 2963–2972.
[3] J. Robinson, V. Liang, J. Champers, C. MacKenzie, Computer user verification using login string keystroke dynamics, IEEE Transactions on System, Man and Cybernetics—Part A 28 (2) (1998) 236–241.
[4] A. Peacock, K. Xian, M. Wilkerson, Typing patterns: a key to user identification, IEEE Security & Privacy 2 (5) (2004) 40–47.
[5] M. Tanaka-Yamawaki, Human generated random numbers and a model of the human brain functions, in: Proceedings of the IEEE SMC '99, vol. 3, Tokyo, Japan, 1999, pp. 223–228.
[6] N. Persaud, Humans can consciously generate random number sequences: a possible test for artificial intelligence, Medical Hypotheses 65 (2) (2005) 211–214.
[7] G. Madison, Fractal modeling of human isochronous serial interval production, Biological Cybernetics 90 (2) (2004) 105–112.
[8] P. Brugger, A.U. Monsch, D.P. Salmon, N. Butters, Random number generation in dementia of the Alzheimer type: a test of frontal executive functions, Neuropsychologia 34 (2) (1996) 97–103.
[9] B. Kay, E. Saltzman, J. Kelso, G. Schöner, Space–time behavior of single and bimanual rhythmical movements: data and limit cycle model, Journal of Experimental Psychology: Human Perception and Performance 13 (2) (1987) 178–192.
[10] V. Jirsa, A. Fuchs, J. Kelso, Connecting cortical and behavioral dynamics: bimanual coordination, Neural Computation 10 (8) (1998) 2019–2045.
[11] J. Kelso, Dynamics Patterns: The Self-organization of Brain and Behavior, MIT Press, Cambridge, MA, 1995.
[12] K. Jantzen, F. Steinberg, J. Kelso, Brain networks underlying human timing behavior are influenced by prior context, PNAS 101 (17) (2004) 6815–6820.
[13] ⟨http://www.thecomplementarynature.com/TCN_Movies.php⟩.
[14] N. Jimeno, A. Jimeno, R. Hornero, A. Alonso, P. Espino, The test of random rhythm generation and neuropsychological performance in schizophrenic patients, Neurology Psychiatry and Brain Research 7 (3) (1999) 137–142.
[15] R. Hornero, A. Alonso, N. Jimeno, A. Jimeno, M. Lopez, Nonlinear analysis of time series generated by schizophrenic patients, IEEE Engineering in Medicine and Biology 18 (3) (1999) 84–90.
[16] R. Hornero, D. Abasolo, N. Jimeno, C. Sanchez, J. Poza, M. Aboy, Variability, regularity, and complexity of time series generated by schizophrenic patients and control subjects, IEEE BME 53 (2) (2006) 210–218.
[17] H. Abarbanel, Analysis of Observed Chaotic Data, Springer, New York, 1996.
[18] C. Theoharatos, N. Laskaris, G. Economou, S. Fotopoulos, A generic scheme for color image retrieval based on the multivariate Wald-Wolfowitz test, IEEE Transactions on Knowledge and Data Engineering 17 (6) (2005) 808–819.
[19] J. Friedman, L. Rafsky, Graphics for the multivariate two-sample problem, Journal of the American Statistical Association 76 (374) (1981) 277–287.
[20] F. Takens, Detecting strange attractors in turbulence, in: Dynamical Systems and Turbulence, Lecture Notes in Mathematics, vol. 898, Springer, Berlin, 1981, pp. 366–381.
[21] G. Simon, A. Lendasse, M. Cottrell, J.-C. Fort, M. Verleysen, Double quantization of the regressor space for long-term time series prediction: method and proof of stability, Neural Networks 17 (8–9) (2004) 1169–1181.
[22] G. Simon, J. Lee, M. Verleysen, Unfolding preprocessing for meaningful time series clustering, Neural Networks 19 (6–7) (2006) 877–888.
[23] T.W. Liao, A clustering procedure for exploratory mining of vector time series, Pattern Recognition 40 (9) (2007) 2550–2562.
[24] M. Ramoni, P. Sebastiani, P. Cohen, Bayesian clustering by dynamics, Machine Learning 47 (1) (2002) 91–121.
[25] N. Laskaris, A. Ioannides, Exploratory data analysis of evoked response single trials based on minimal spanning tree, Clinical Neurophysiology 112 (3) (2001) 698–712.
[26] N. Laskaris, A. Ioannides, Semantic geodesic maps: a unifying geometrical approach for studying the structure and dynamics of single trial evoked responses, Clinical Neurophysiology 113 (8) (2002) 1209–1226.
[27] S. Yan, D. Xu, B. Zhang, H.J. Zhang, Q. Yang, S. Lin, Graph embedding and extensions: a general framework for dimension analysis reduction, IEEE Transactions on Pattern Analysis and Machine Intelligence 28 (1) (2007) 40–51.
[28] S. Zafeiriou, A. Tefas, I. Pitas, Minimum class variance support vector machines, IEEE Transactions on Image Processing 16 (10) (2007) 2551–2564.
[29] J. Gower, Adding a point to vector diagrams in multivariate analysis, Biometrica 55 (3) (1968) 582–585.
[30] Y. Bengio, J.F. Paiement, P. Vincent, O. Delalleau, Out-of-sample extensions for LLE, isomap, MDS, eigenmaps, and spectral clustering, Advances in Neural Information Processing Systems 16 (2004).
[31] I. Borg, P. Groenen, Modern Multidimensional Scaling, Springer, New York, 1997.
[32] P. Good, Permutation Tests, Springer, New York, 2000.

[33] V. Vapnik, Statistical Learning Theory, Wiley, New York, 1998.
[34] B. Scholkopf, A. Smola, Learning with Kernels, MIT Press, Cambridge, MA, 2002.
[35] C. Kotropoulos, A. Tefas, I. Pitas, Frontal face authentication using discriminating grids with morphological feature vectors, IEEE Transactions on Multimedia 2 (1) (2000) 14–26.
[36] C. Kotropoulos, A. Tefas, I. Pitas, Morphological elastic graph matching applied to frontal face authentication under well-controlled and real conditions, Pattern Recognition 33 (12) (2000) 31–43.
[37] A. Tefas, C. Kotropoulos, I. Pitas, Using support vector machines to enhance the performance of elastic graph matching for frontal face authentication, IEEE Transactions on Pattern Analysis and Machine Intelligence 23 (7) (2001) 735–746.
[38] S. Zafeiriou, A. Tefas, I. Pitas, Learning discriminant person specific facial models using expandable graphs, IEEE Transactions on Information Forensics and Security 2 (1) (2007) 55–68.
[39] K.N. Plataniotis, D. Hatzinakos, J. Lee, ECG biometric recognition without fiducial detection, in: Proceedings of the Biometric Consortium Conference, September 2006, pp. 1–6.
[40] L. Biel, O. Pettersson, L. Philipson, P. Wide, ECG analysis: a new approach in human identification, IEEE Transactions on Instrumentation and Measurement 50 (3) (2001) 808–812.
[41] S.A. Israel, J.M. Irvine, A. Cheng, M.D. Wiederhold, B.K. Wiederhold, ECG to identify individuals, Pattern Recognition 38 (1) (2005) 138–142.
[42] J.M. Irvinr, S.A. Israel, W.T. Scruggs, W.J. Worek, EigenPulse: robust human identification from cardiovascular function, Pattern Recognition 41 (11) (2008) 3427–3435.
[43] A.D. Chan, M.M. Hamdy, A. Badre, V. Badee, Person identification using electrocardiograms electrical and computer engineering, in: Proceedings of the CCECE'06, May 2006, pp. 1–4.
[44] F. Beritelli, S. Serrano, Biometric identification based on frequency analysis of cardiac sounds, IEEE Transactions on Information Forensics and Security 2 (3 Part 2) (2007) 596–604.
[45] S. Marcel, J. Millan, Person authentication using brainwaves (EEG) and maximum a posteriori model adaptation, IEEE Transactions on Pattern Analysis and Machine Intelligence 29 (4) (2007) 743–752.
[46] R. Palaniappan, D.P. Mandic, Biometrics from brain electrical activity: a machine learning approach, IEEE Transactions on Pattern Analysis and Machine Intelligence 29 (4) (2007) 738–742.
[47] K. Ueno, X. Xi, E. Keogh, D.-J. Lee, Anytime classification using the nearest neighbor algorithm with applications to stream mining, in: Proceedings of the ICDM'06, 2006, pp. 623–632.
[48] R. Brooks, T. Arbela, D. Precup, Anytime similarity measures for faster alignment, Computer Vision and Image Understanding 110 (3) (2008) 378–389.

About the Author—NIKOLAOS LASKARIS received both the M.S. degree (1995) and Ph.D. degree (1998) from Patras University, Greece. He joined the Laboratory for Human Brain Dynamics in RIKEN-BSI, Japan (1999–2003). Currently, he is a Faculty Member of Informatics Department in AUTH, Greece and his research interests include computational intelligence, soft computing, data mining and their applications in biomedicine and neuroscience.

About the Author—STEFANOS ZAFEIRIOU received both the B.Sc. degree in Informatics (2003) and the Ph.D. (2007) from the Aristotle University of Thessaloniki, Greece. He has co-authored more than 30 scientific publications. He is currently with the Communications and Signal Processing Group at the Department of Electrical and Electronic Engineering of Imperial College and his main research interests lie in the development and applications of computational intelligence methodologies.

About the Author—LAMBRINI GAREFA received the M.S. degree (2008) in Informatics from the Aristotle University of Thessaloniki, Greece. Her main research interests lie in the applications of computational intelligence methodologies on biological data sets.